Simulation of Energy Absorption in Braided Composite Tubes through Axial Crushing

Carla McGregor[a], Reza Vaziri[a], and Xinran Xiao[b]

[a]*Composites Group, Departments of Civil Engineering and Materials Engineering, The University of British Columbia, Vancouver, B.C., Canada, V6T 1Z4*
[b]*General Motors Corporation, Research & Development, MC 480-106-710, 30500 Mound Road, Warren, MI 48090-9055*

Abstract

Modeling damage propagation and energy absorption in composite tubular structures under axial compression is a challenging task due to the complex nature of damage growth in composites. In this paper, our model (CODAM for COmposite DAMage), which is incorporated into LS-DYNA® as a user material model, is used to simulate the axial crushing response of braided composite tubes. Recent improvements to the finite element model include the addition of a debris wedge, representation of delamination using a tiebreak contact interface, and more physically based model parameters. It is shown that the damage propagation, fracture morphology and energy absorption predictions correlate well with the experimental results.

Introduction

Braided composite tubular structures are of interest as feasible energy absorbing components in vehicular front rail structures to improve crashworthiness [1-3]. Finite element models capable of simulating damage propagation and absorption in these materials are needed to efficiently design and incorporate such structures into vehicles. This is a challenging task given the complex damage mechanisms, such as fiber fracture, matrix cracking, kink banding, and delamination that are characteristic of composites, as well as the lack of accurate and robust predictive numerical tools.

Modeling attempts in this area have focused on representing the response of the braided composite at either the micromechanical (at the constituent level) or macromechanical level (at the lamina or laminate level). Both approaches have their own advantages and challenges. Micromechanical approaches have the potential to represent the behaviour and interactions of the constituents, and the resulting response of the braid very accurately. However, the resulting models tend to be fairly complex and inefficient when attempting to model full scale dynamic tube crushing events. Moreover, accurate characterization of the constituents and interaction through all stages of damage is challenging in itself. Macromechanical approaches are much more feasible in terms of computational efficiency, but maintaining a physical basis to the models can be challenging. Additionally, details of the fracture process can be lost in the smearing approach.

Beard and Chang [4,5] used a micromechanical model incorporated as a subroutine into the ABAQUS implicit code to simulate the complete crushing process of triaxially braided composite tubes with promising initial results. In the model, at each increment, the strain state of the Representative Unit Cells (RUC's) are passed to a subroutine that calculate the degradation

of the mechanical properties of the tows and resin pockets. The subroutine then returns the updated stress state of the RUC to the model in ABAQUS. The model was later incorporated into ABAQUS/Explicit and used to model dynamic tube crushing events by Flesher [6].

Our model (CODAM for COmposite DAMage), which is incorporated into LS-DYNA® as a user material model is a continuum damage mechanics based macromechanical model for composite materials [7,8]. The model has shown promise in predicting the crushing response of braided tubes [9]. This study focuses on improving the model predictions. Refinements to the model include the addition of a debris wedge, a distinguishing feature in tubes displaying a splaying mode of failure, and representation of delamination using a tiebreak contact interface that allows energy absorption through the un-tying process. Model parameters defining the material and delamination response are related to experimentally observed behavior and the resulting damage propagation, fracture morphology and energy absorption predictions correlate well with the experimental results. This paper will present the details of the model and the comparisons between the predicted and experimental tube crushing responses.

Material and Experimental Details

Two ply and four ply braided tubes having lengths of approximately 360 mm supplied by General Motors Corporation were tested in a 10 kJ drop tower facility at the University of British Columbia (Figure 1). The tubes were made of Fortafil #556 80k[1] carbon axial tows and Grafil 34-700 12k carbon biaxial tows in an Ashland Hetron 922 resin with each ply having a [0/±45] braid architecture. All tubes were machined at one end to form a 45° chamfer to encourage progressive crushing. Basic properties of the two tube geometries are summarized in Table I. Additional material properties can be found in Appendix A.
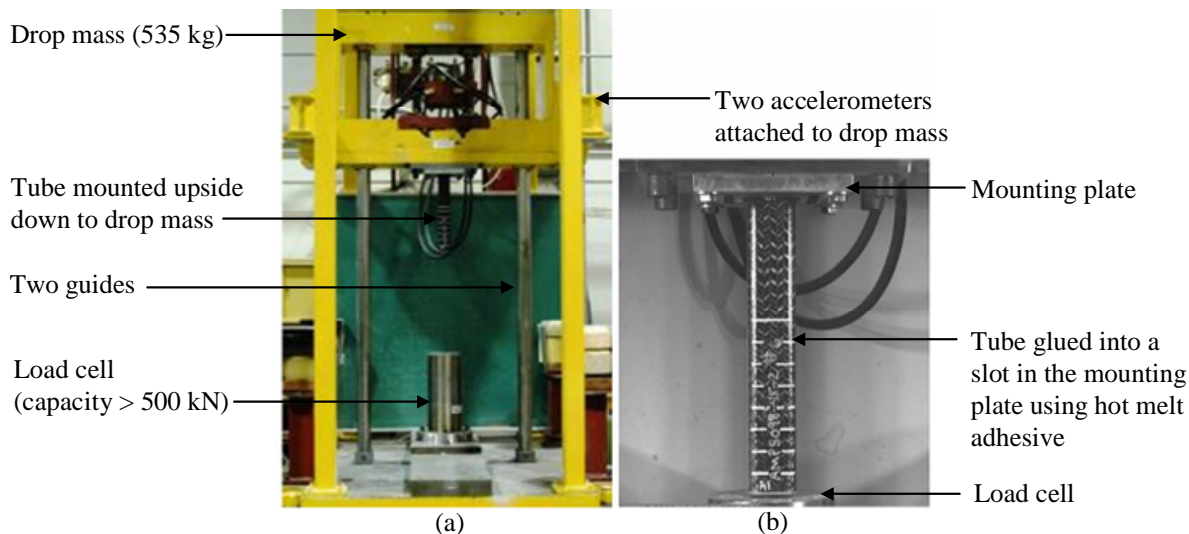
Figure 1   (a) Photograph of drop tower test set-up and (b) video image showing a 2-ply tube just prior to impact with the load cell.

---

[1] An 80k tow is composed of 80,000 individual fibres

Table I
Test matrix of braided tubes crushed without an external plug initiator

Nominal Outside Geometry (mm)	Braid	Number of tests	Drop mass (kg)	Drop height (m)	Impact velocities* (m/s)	Range of impact kinetic energy* (kJ)
55 × 55	[0/±45]₂	7	535	3 @ 0.50	3 @ 3.1	3 @ 2.6
				3 @ 1.00	3 @ 4.4	3 @ 5.3
55 × 55	[0/±45]₄	6	535	3 @ 1.00	3 @ 4.4	3 @ 5.2
				1 @ 1.47	1 @ 5.4	1 @ 7.7
				3 @ 1.90	2 @ 6.1	2 @ 10.1

* Theoretical values calculated from measured drop height and mass of 535 kg are reported. Actual values are less than these due to energy losses such as friction along the guides.

The fracture morphology of the tubes was characterized by the development of a main delamination front, which caused some plies to bend inwards and some to bend outwards, as illustrated in Figure 2. The main driving mechanism behind this splitting is a debris wedge (Figure 3) that forms early in the crushing process. This debris wedge is a collection of pulverized material that forms at the bottom of the tube and plays a key role in promoting stable progressive crushing, as well as in energy absorption via friction.

In plies bending outward, transverse tensile fracture, which was moderately localized to the four corners, was the main mode of damage. This tearing led to the fracture of the biaxial braider tows and the separation of the axial tows. Damage was also introduced to the four external fronds of the tube due to bending. Fibre breakage due to tensile bending strains in the axial tows was not very significant while delaminations between all plies were. The plies bending inward also experienced bending induced damage as well as damage caused by compaction and contact between plies inside the tube.

    (a)   (b)   (c)   (d)
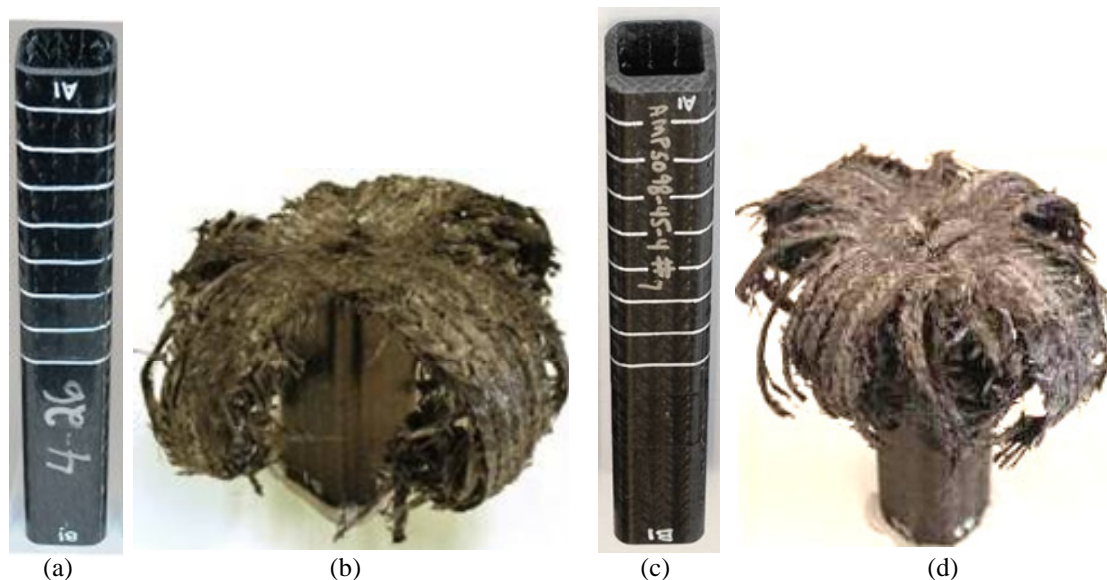
Figure 2   Photographs of the (a,c) pre-tested tubes and (b,d) resulting typical fracture morphologies observed in the 2-ply (shown on the left) and 4-ply (shown on the right) tubes.

(a)   (b)
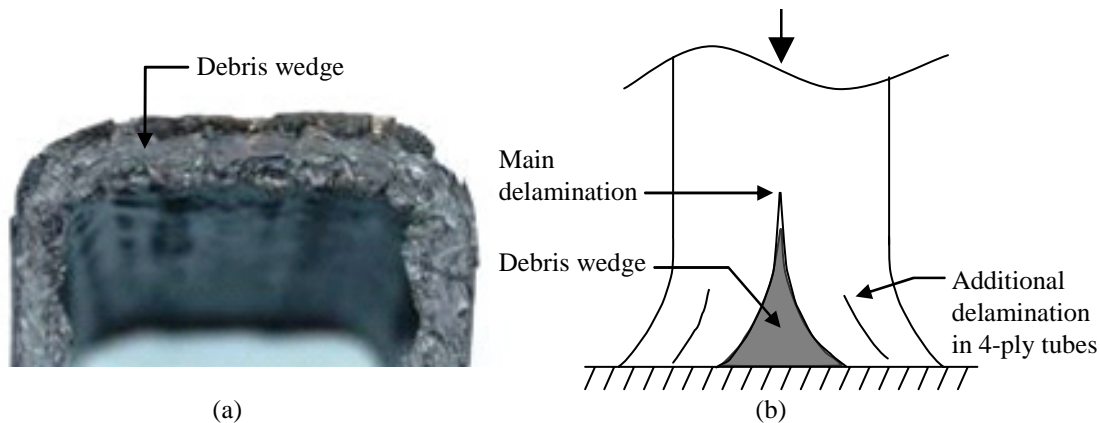
Figure 3   (a) Top view of $[0/\pm45]_2$ tube showing the formation of the debris wedge after approximately 5 mm of applied displacement and (b) schematic showing the debris wedge and fracture mechanisms in a section of the tube wall.

Finite Element Model

The LS-DYNA simulations consisted of 4 main components: a drop weight, a tube, a debris wedge and a rigid plate as shown in Figure 4. Due to symmetry, only a quarter of the tube was modeled. The drop weight was modeled as a rigid body with a mass equal to ¼ of the total 535 kg drop mass. The tube material behavior was governed by the CODAM constitutive model. The rigid plate was modeled as a rigid body with a modulus of 210 GPa fixed in space. The debris wedge was modeled using solid elements as a rigid body with a modulus of 5 GPa fixed in space. It is acknowledged that having the debris wedge present through-out the duration of crushing does not accurately represent the beginning stages of crush, over which the debris wedge is developing. Thus, the final LS-DYNA predictions are a combination of a simulation without the debris wedge (to capture the first few millimeters of crushing) and a simulation with the debris wedge (to capture the remaining response).

Initial velocities of 3.8 and 4.9 m/s were assigned to the drop weight and tube in the 2-ply and 4-ply simulations, respectively. Gravitational force was also represented (using the Load_Body option in LS-DYNA) to properly capture the potential energy of the system.

Delamination between all plies was modeled using the built-in "tie-break" interface option (*CONTACT_AUTOMATIC_ONE_WAY_SURFACE_TO_SURFACE_TIEBREAK). This contact represents surfaces initially tied together that will eventually release, absorbing energy through the process. Contact between the tube and the debris wedge and rigid wall were modeled using *CONTACT_AUTOMATIC_SURFACE_TO_SURFACE. A coefficient of friction of 0.35 was used between the tube and the rigid wall based on values measured by DeTeresa *et al.* [10] in friction tests. A higher value of 0.40 was assumed for contact between the tube and the debris wedge due to the highly abrasive nature of the debris wedge.

To represent the interaction of the plies inside the tube (between the plies bending inward in the quarter tube model and those from the remaining ¾'s of the tube not represented in the model), two planar, finite rigid walls running up the length of the tube were defined (Figure 4). The

coefficient of friction was assumed to be equal to 0.40 (again due to the highly abrasive nature of the material within the tube).

The option to erode elements, thus removing them completely from the analysis was also active in all simulations. Erosion is helpful when a strain-softening material model is defined because degraded elements can distort easily, leading to high hourglass energy requirements and visually disturbing results. The erosion criterion, which was based on total strain, was set such that only fully damaged elements were removed from the simulation.
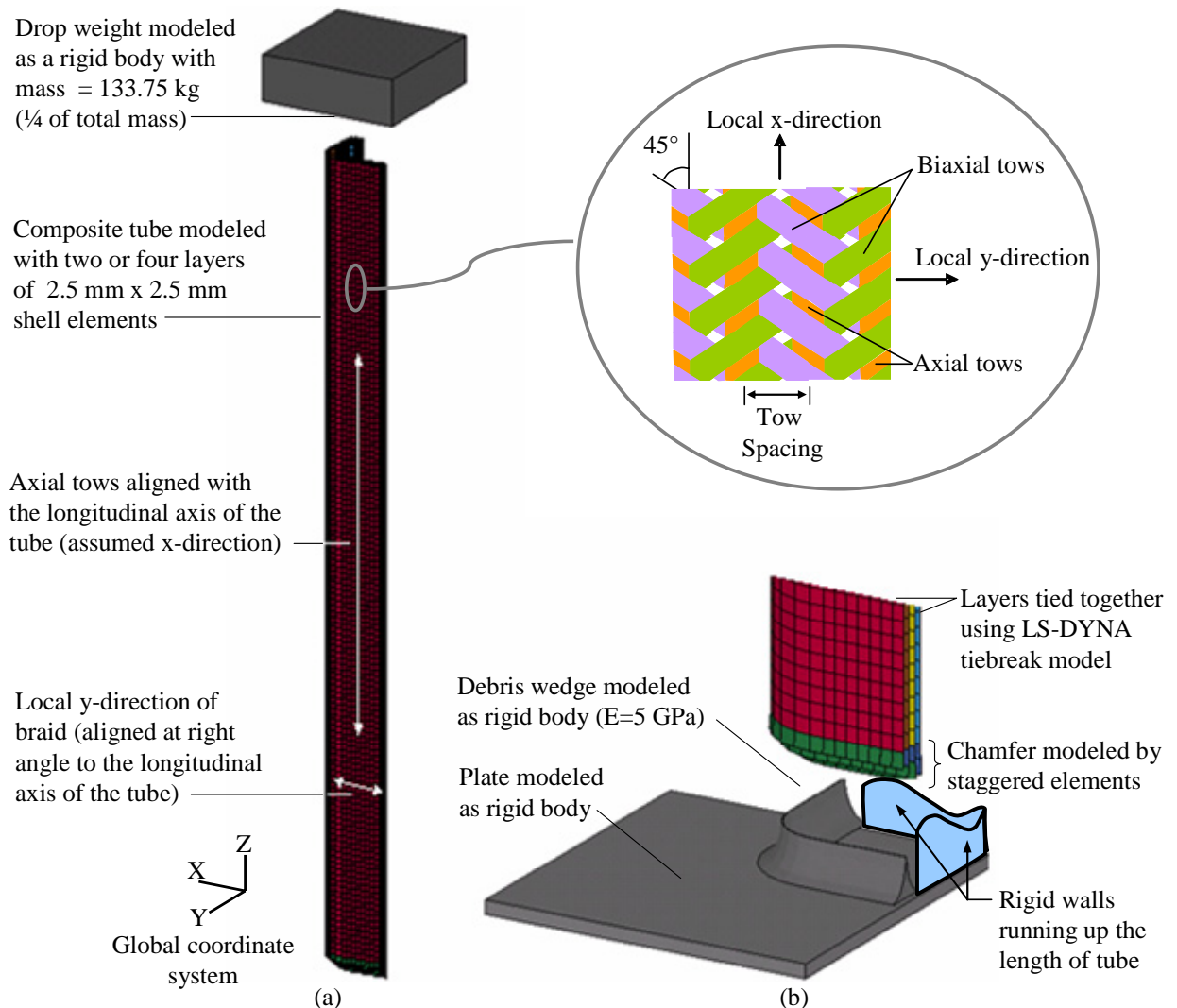
Figure 4   Schematic of the basic components in the tube simulation. The tube contacts the rigid plate. The debris wedge that forms during the initial stages of crushing is represented by a rigid body present at the start of the simulation.

Constitutive Model

CODAM (COmposite DAMage) is implemented as a user material model into the explicit finite element analysis program, LS-DYNA, and represents the tensile and compressive constitutive behavior of composite laminates through both the pre-failure (elastic) and post-initial failure regimes. In essence, it is a strain-softening material model that computes and tracks the damage state and corresponding degradation of material properties (moduli) of an element based on its current and past strain states.

It has been demonstrated that strain-softening material models are prone to mesh dependent behavior [11]. As an element size decreases, so does the associated energy absorption. With CODAM, the stress-strain response is defined at the level of the Representative Volume Element (RVE). The RVE dimensions correspond to the finite size over which distributed cracking and damage accumulates in the quasi-brittle material, when tested under conditions that lead to stable damage growth. A crack band scaling [11] is implemented in CODAM [8] to account for element sizes that are not equal to the characteristic RVE size. In the tube crushing simulations, the element size of 2.5 mm is less than the RVE dimensions of approximately 15 mm (compression in the local x-direction) and 18 mm (tension in the local y-direction).

Figure 5 shows the stress-strain profile that represents the RVE response of the 2-ply braid. The transverse tensile response was determined from Over-height Compact Tension tests. Compressive damage through band-broadening in the longitudinal direction is represented by a plateau stress (value of the plateau stress is taken to be the compressive strength obtained from analysis of 4-point bend). Transverse compression and longitudinal tension were assumed to remain elastic due to their insignificant role in the tube crushing response.

Coupon testing as well as visual inspection indicated that the 4-ply material was of better quality than the 2-ply material. For example, in the OCT tests, the measured transverse tensile fracture energy was approximately 15% higher in the 4-ply specimens. To capture this in the simulations, the moduli, fracture energy and plateau stress were all increased by 15% in the 4-ply material model.

(a)

(b)
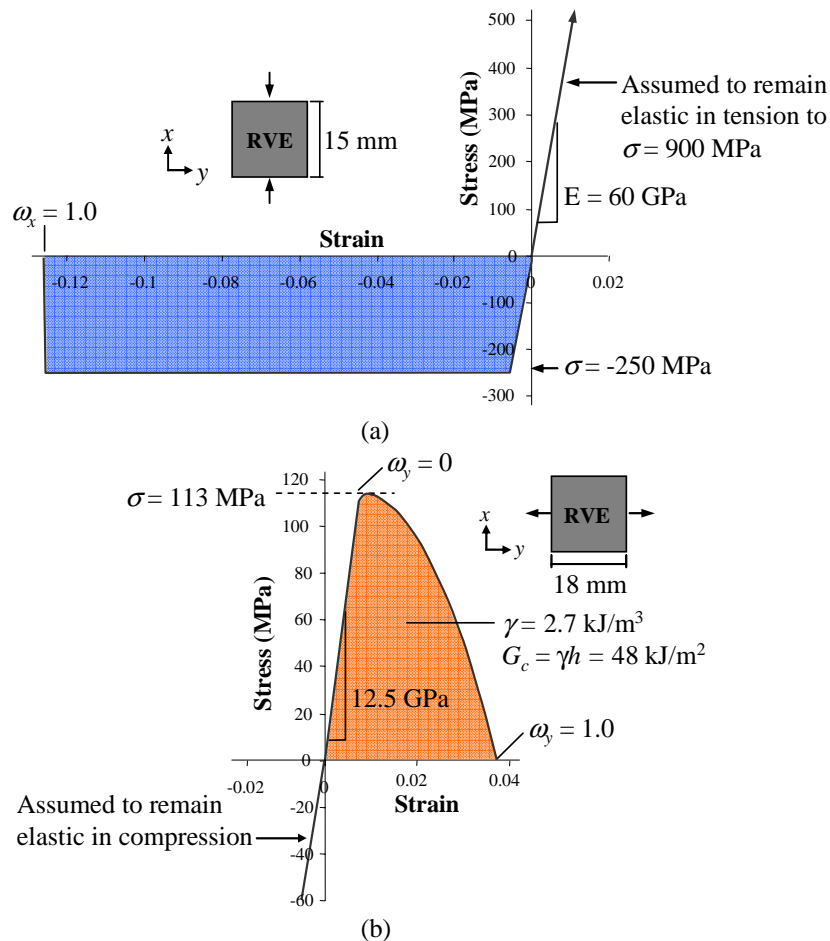
Figure 5   Input stress-strain response in the (a) local x-direction (longitudinal) and (b) local y-direction (hoop) for the 2-ply braided material.

Simulation Results

The two tube configurations were simulated under axial crushing conditions in LS-DYNA and the resulting predictions were compared to experimental results using the following measures:
- Fracture morphology
- Force-displacement profiles
- Load ratio values
- Specific Energy Absorption (SEA) values

Figure 6 shows the main features of fracture in the 2-ply [0/±45] tube simulation. The inner ply bends towards the inside of the tube and the outer ply bends outwards. The central delamination is driven by the presence of the debris wedge. The response of the 4-ply tube is very similar, with the addition of delamination between the additional plies. Analogous to the experiments, the simulations predict that damage is introduced via transverse tearing at the corners and axial damage accumulation due to bending. The plies that bend inward are also accumulating damage as they are forced over the debris wedge and impacting the rigid wall. The predicted fracture morphologies compare well to that observed experimentally.
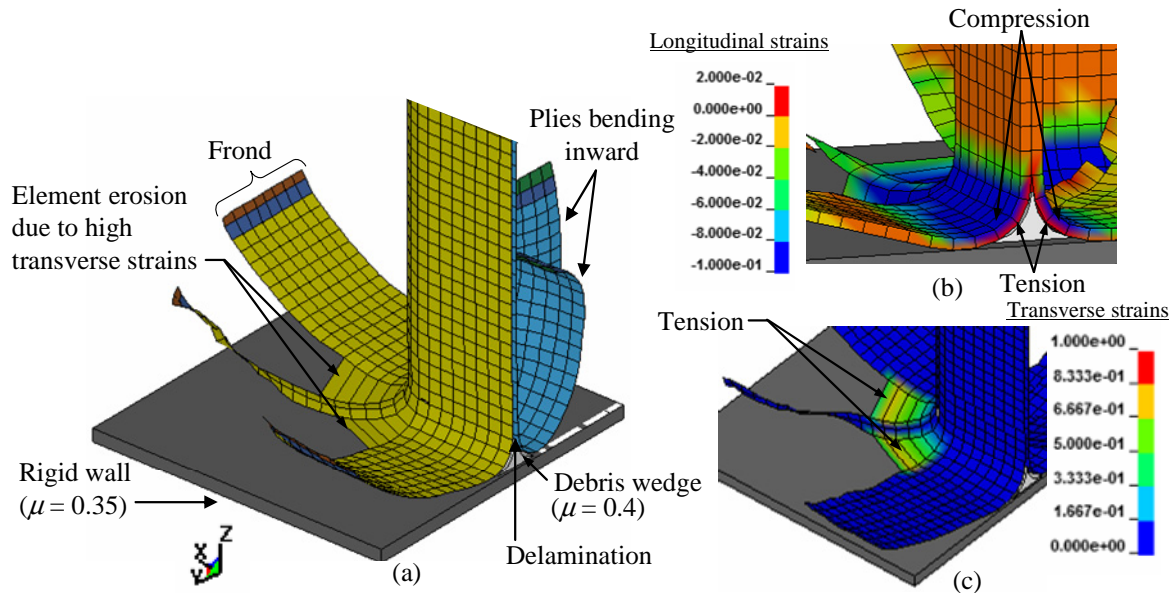
Figure 6   2-ply [0/±45] tube after approximately 50 mm of displacement, showing (a) overall fracture morphology (b) axial tensile and compressive strains due to bending (shown with thickness option in LS-DYNA) and (c) transverse tensile strains due to tearing at the corners.

The predicted 2-ply force-displacement profile (loads measured from the contact forces in LS-DYNA) is compared to the crushing loads measured from two of the tubes tested in the drop tower in Figure 7. The LS-DYNA load-displacement trace is a combination of the results from the simulation without the debris wedge (axial displacements $\delta < 7$ mm) and the simulation with the debris wedge ($7 < \delta < 206$ mm). The simulation results agree well with the experiments, with the exception of the zone between 7 mm and 12 mm, where the loads are under-predicted.
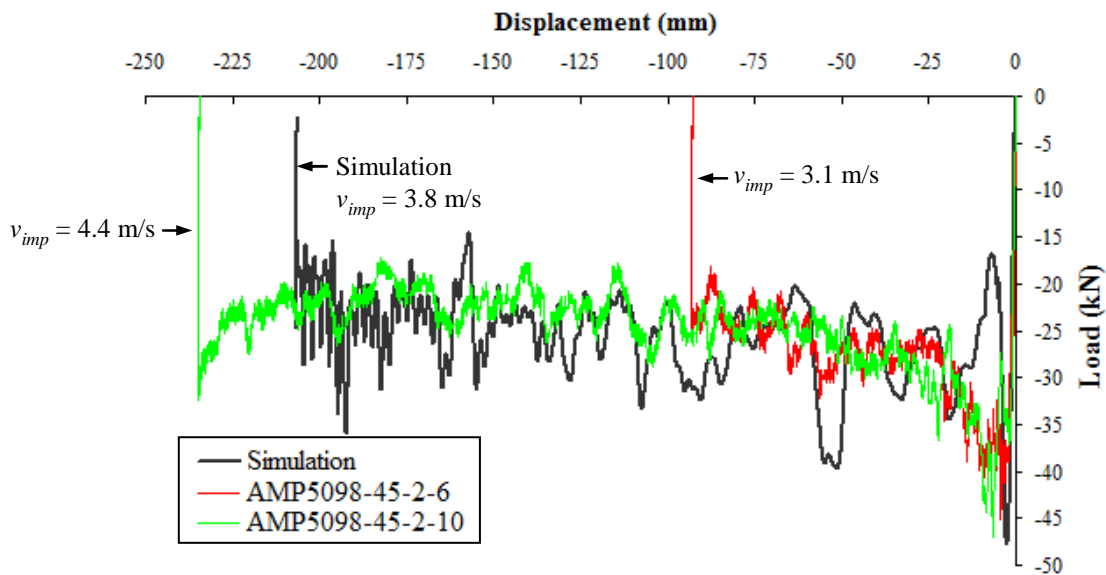
Figure 7   Comparison of predicted 2-ply load-displacement profile to two experimental profiles. The first 7 mm of the LS-DYNA results are from the simulations without the debris wedge.

Energy absorption efficiency of the tubes can be evaluated by studying the damage induced through crushing. This can be accomplished by studying the elemental damage parameters, ω_x and ω_y. Damage parameters range from zero (indicating no damage) to one (indicating complete damage). The level and distribution of predicted damage in the tube during crushing is shown in Figure 8 for the outer ply of the 2-ply tubes using fringe plots of the elemental damage parameters (ω_x and ω_y). The dominant modes of damage are axial compressive and transverse tensile damage. The 4-ply tubes showed very similar distributions.
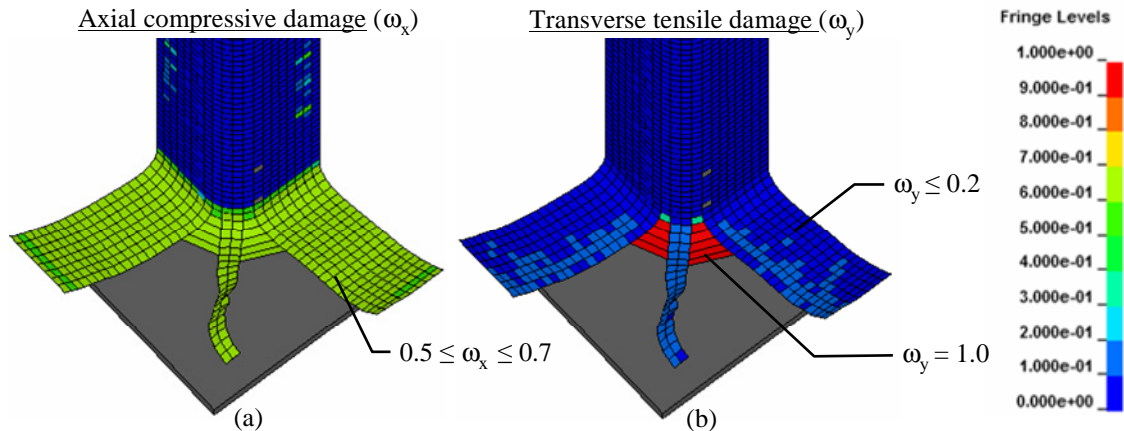
Figure 8   Fringe plots of (a) axial compressive damage parameter (ω_x) and (b) transverse tensile damage parameter (ω_y) in the outermost ply of the 2-ply tube. In the axial direction, fringe plot is shown for the upper surface (which is in compression due to bending).

The 4-ply force-displacement profile predicted by LS-DYNA is shown in Figure 9. Again, this profile is a combination of a simulation without the debris wedge ($0 < \delta < 7$ mm) and a simulation with the debris wedge ($7 < \delta < 206$ mm). The simulation results once again agree relatively well with the measured experimental results.

A comparison between the predicted and experimental values of the overall specific energy absorption (SEA) and load ratio (ratio of peak to average load) is shown in Figure 10. The predicted SEA values of 41 and 46 J/g for the 2-ply and 4-ply tubes, respectively, agree very well with the experimental average values of 43 and 46 J/g. Given the challenge associated with accurately capturing the development of the debris wedge in the model, the predicted load ratio values agree relatively well with the experiments.
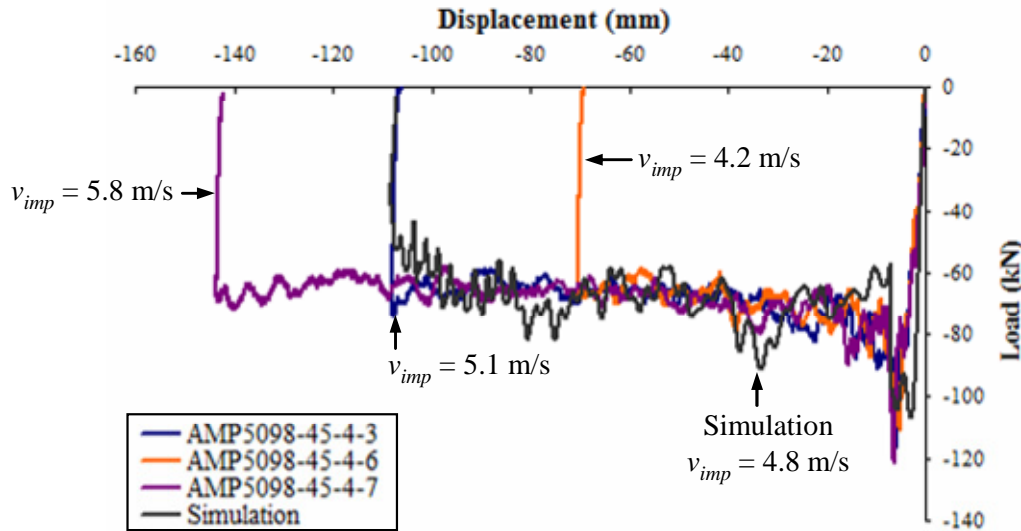
Figure 9   Comparison of predicted 4-ply load-displacement profile to three experimental profiles. The first 7 mm of the LS-DYNA results are from the simulations without the debris wedge.
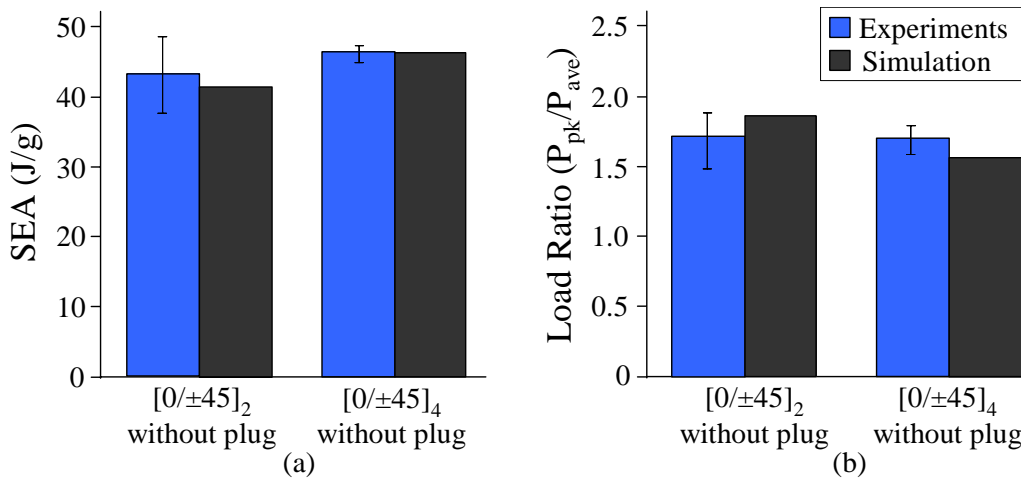
Figure 10   Comparison of predicted and experimentally measured values of (a) SEA and (b) load ratio. Upper and lower experimental bounds are represented by the error bars.

In LS-DYNA, the various components of both the energy supplied to the system (impact energy) and the energy ultimately absorbed and dissipated by the system can be measured and categorized, as shown in Figure 11. The impact energy has both a kinetic and a potential component to it. In terms of energy absorption, the relative compartmentalization is very similar between the two tubes. The least significant source of energy absorption is through delamination, accounting for less than 2% of the total energy absorbed. However, this aspect of the simulation is vital to capturing the correct fracture morphology. The majority of the energy is absorbed through material fracture and damage, however, friction (between the tube and the rigid wall and between the tube and debris wedge) also accounts for a large portion (approximately 35% of the total energy absorbed).
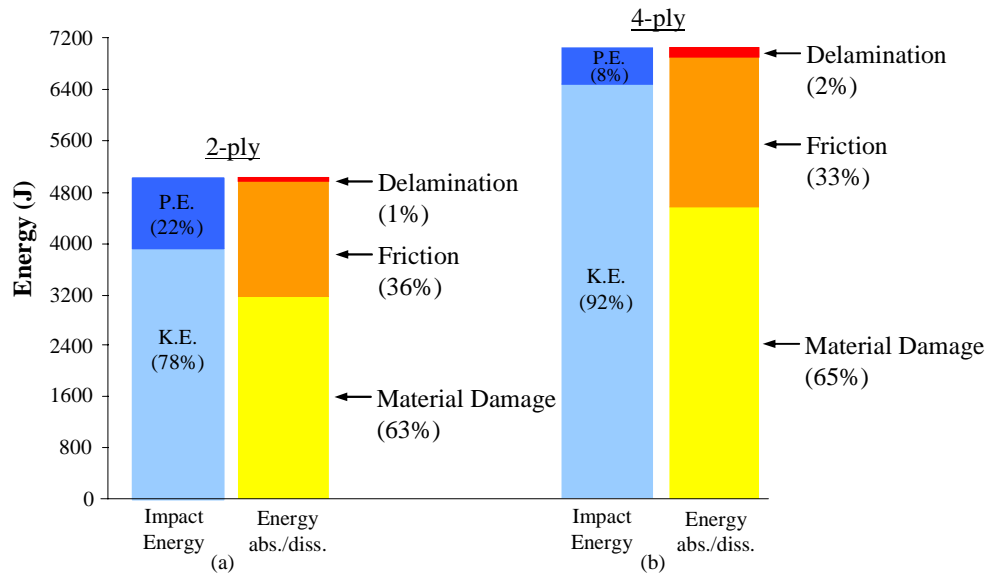
Figure 11   Schematic showing how the energy supplied to the system (as Potential Energy and Kinetic Energy) is absorbed and dissipated through various processes in (a) the 2-ply tube and (b) the 4-ply tube. In both cases, the majority of the energy is absorbed through material damage.

Summary

Dynamic crushing of the 2-ply and 4-ply composite tubes under varying impact energy levels was carried out on a drop tower facility at the University of British Columbia. The testing was successful in that the SEA, peak load, and load ratio values were determined and compared. In terms of SEA and load ratio, the thicker tubes performed slightly better than the thinner tubes.

The damage propagation, force-displacement profile, and specific energy absorption trends predicted by LS-DYNA agreed well with the experiments. The debris wedge, which develops experimentally at the bottom of the tube, was represented in the model as a solid rigid body that is fixed, both dimensionally and spatially. This oversimplification does not accurately represent the mechanics of the wedge. However, the enhancements to the model (presence of the debris wedge and delamination capabilities between the plies) result in major improvements over past attempts to model braided composite tubes crushed without a plug initiator (See [9]). In these previous models, stability of the simulation was a major issue, often resulting in premature termination of the simulation. Additionally, the predicted fracture morphology did not agree well with experiments.

The success of this study suggests that there is an opportunity to use LS-DYNA as a design aid for future incorporation of lightweight composite energy absorbers into crashworthy structures. Additionally, this study improves the confidence in using CODAM as a predictive tool to simulate the effect of damage in composites subjected to either tensile or compressive loads.

Acknowledgements

References

[1]   Chiu,C.H., Tsai,K.-. and Huang,W.J., "Effects of Braiding Parameters on Energy Absorption Capability of Triaxially Braided Composite Tubes," Journal of Composite Materials, vol. 32, pp. 1964-1983, 1998.

[2]   Karbhari,V.M. and Haller,J.E., "Rate and Architecture Effects on Progressive Crush of Braided Tubes," Composite Structures, vol. 43, pp. 93-108, 1998.

[3]   Queck,S.C., Waas,A.M., Hoffman,J. and Agaram,V., "The Cruishing Response of Braided and CSM Glass Reinforced Composite Tubes," Composite Structures, vol. 52, pp. 103-112, 2001.

[4]   Beard,S.J. and Chang,F.K., "Energy Absorption of Braided Composite Tubes," International Journal of Crashworthiness, vol. 7, pp. 191-206, 2002.

[5]   Beard,S. and Chang,F., "Design of Braided Composites for Energy Absorption," Journal of Thermoplastic Composite Materials, vol. 15, pp. 3-12, 2002.

[6]   Flesher,N.D. "Crash Energy Absorption of Braided Composite Tubes," Ph. D Thesis, Department of Mechanical Engineering, Stanford University, Stanford, CA, USA, 2006.

[7]   Williams,K.V., Vaziri,R. and Poursartip,A., "A Physically Based Continuum Damage Mechanics Model for Thin Laminated Composite Structures," International Journal of Solids and Structures, vol. 40, pp. 2267-2300, 2003.

[8]   Floyd,A.M. "An Engineering Approach to the Simulation of Gross Damage Development in Composite Laminates," Ph.D. Thesis, Department of Civil Engineering, The University of British Columbia, Vancouver, BC, Canada, 2004.

[9]   McGregor,C. "Simulation of Progressive Damage Development in Braided Composite Tubes Under Axial Compression," M.A.Sc. Thesis, Department of Civil Engineering, The University of British Columbia, Vancouver, BC, Canada, 2005.

[10]   DeTeresa,S.J., Allison,L.M., Cunningham,B.J., Freeman,D.C., Saculla,M.D., Sanchez,R.J. and Winchester,S.W., "Experimental results in support of simulating progressive crush in carbon-fiber textile composites," UCRL-ID-143287, Lawrence Livermore National Laboratory, 7000 East Avenue, Livermore, CA 94550, March 12, 2001.

[11]   Z. P. Bazant and J. Planas, Fracture and Size Effect in Concrete and Other Quasibrittle Materials. CRC Press, 1998.

Appendix A: Material Properties

Table II
Manufacturer's Material Properties

Property	Grafil 34-700 12k[2]	Fortafil #556 80k[3]	Hetron 922[4]
Number of Filaments	12,000	80,000	-
Strength (MPa)	4820	3790	86.2
Modulus (GPa)	234	231	3.17
Density (g/cm^3)	1.80	1.80	1.14
Tow x-sectional Area (mm^2)	0.444	2.34	-
Elongation at yield (%)	-	-	4.9
Elongation (%)	2	1.64	6.7
Filament Diameter (μm)	7	6	-

Table III
Basic properties of two tube architectures.

	Tube A	Tube B
Braid architecture	[0/±45]	[0/±45]
Number of plies	2	4
Number of Filaments in Axial Tow	80,000	80,000
Number of Filaments in Braider Tow	12,000	12,000
Average Wall Thickness (mm)	2.3	6.1
Average density (g/cm^3)	1.33	1.28
Axial tow spacing (mm)	8.39	8.39
Cross-sectional area (mm^2)	470	1163
Axial* Tensile Modulus (GPa)	64.7	-
Axial* Compressive Modulus (GPa)	53	-
Transverse* Tensile Modulus (GPa)	10	-
Transverse* Compressive Modulus (GPa)	14.4	-

* Moduli values taken from coupon tests done by Huang and Waas [12] (axial direction is aligned with the 0° tows and transverse direction is perpendicular to this).

---

[2] http://www.grafil.com/

[3] Akzo Nobel recently acquired by Toho Tenax Inc. (http://www.tohotenaxamerica.com/)

[4] http://www.ashland.com/